NACA RM L53D20

NACA

RESEARCH MEMORANDUM

FLIGHT-DETERMINED PRESSURE DISTRIBUTIONS OVER THE WING

OF THE BELL X-1 RESEARCH AIRPLANE (10-PERCENT-THICK WING)

AT SUBSONIC AND TRANSONIC SPEEDS

By Ronald J. Knapp and Gareth H. Jordan

Langley Aeronautical Laboratory
Langley Field, Va.

CLASSIFICATION CHANGED TO UNCLASSIFIED
AUTHORITY: NACA RESEARCH ABSTRACT NO. 109
EFFECTIVE DATE: NOVEMBER 14, 1956

WHL

NATIONAL ADVISORY COMMITTEE
FOR AERONAUTICS
WASHINGTON

June 29, 1953

CONFIDENTIAL

NATIONAL ADVISORY COMMITTEE FOR AERONAUTICS

RESEARCH MEMORANDUM

FLIGHT-DETERMINED PRESSURE DISTRIBUTIONS OVER THE WING

OF THE BELL X-1 RESEARCH AIRPLANE (10-PERCENT-THICK WING)

AT SUBSONIC AND TRANSONIC SPEEDS

By Ronald J. Knapp and Gareth H. Jordan

SUMMARY

Measurements of chordwise pressure distributions have been made at four spanwise stations over the 10-percent-thick wing of the Bell X-1 research airplane. Data are presented for a range of section normal-force coefficient from -0.20 to 0.80 at Mach numbers from about 0.30 to 1.19.

The results show that the pressure distributions at the four spanwise stations were generally similar at comparable section normal-force coefficients, and that a change occurred from the conventional triangular chordwise loading at low speeds to the more nearly rectangular loading at supersonic speeds. Large changes in the shape of the pressure distributions, with accompanying movement of section center of pressure, occurred at Mach numbers from 0.80 to 0.96 at the midsemispan stations as a result of shock movement with a change in Mach number. The trends of center-of-pressure movement at the root and tip stations were the same as at the midsemispan station, but were not so pronounced because of fuselage and tip effects. At each of the four spanwise stations there was a definitely stable variation of section pitching-moment coefficient with section normal-force coefficient at Mach numbers of 0.89 and above.

At Mach numbers between 0.81 and 0.89, the reduction of pressure recovery behind the shock was greater at the midsemispan stations than at the root or tip stations. This result indicated that separation was more severe at the midsemispan stations.

At a given section normal-force coefficient an approximately constant negative chord-force coefficient existed at subsonic Mach numbers up to somewhat above the critical Mach number at all stations. At transonic Mach numbers a relatively steady increase in chord-force coefficient occurred and continued to a definitely positive value at Mach numbers approaching 1.0, above which the values remained nearly constant to the limit of the tests.

INTRODUCTION

The NACA High-Speed Flight Research Station, Edwards Air Force Base, Calif., has conducted a series of flight tests in the subsonic and transonic speed range with the Bell X-1 research airplane for the measurement of wing loads. The purpose of this paper is to present an analysis of the pressure distributions obtained at the root, tip, and midsemispan stations, together with an analysis of the section aerodynamic-characteristic coefficients (normal-force, pitching-moment, and chord-force) as obtained from the pressure-distribution plots. Most of the data have been presented previously in unanalyzed tabular form in references 1 to 4. The data were obtained for Mach numbers from about 0.30 to 1.19 at altitudes from 17,000 to 47,000 feet in level flight, low-speed stalls, push-overs, and pull-ups to high lift. Relatively complete coverage of this Mach number and normal-force range was made at a station 64.4 percent of the wing semispan from the root. This station was selected as having flow most representative of two-dimensional flow. A portion of the data at this station has previously been analyzed in reference 5. To determine the spanwise variation of the section pressure distributions, less complete tests were made at another midsemispan station, the root station, and the tip station. Some section pressure-distribution data for a midsemispan station of the Bell X-1 research airplane (8-percent-thick wing) are presented in reference 6.

SYMBOLS

$b/2$ wing semispan (14 ft)

C_{N_A} airplane normal-force coefficient, nW/qS

c wing section chord parallel to plane of symmetry, ft

$c_{m_{c/4}}$ section pitching-moment coefficient about the 25-percent-chord point, $\displaystyle\int_0^1 \left(P_U - P_L\right)\left(\frac{x}{c} - \frac{1}{4}\right)d\,\frac{x}{c}$

c_n section normal-force coefficient, $\displaystyle\int_0^1 \left(P_L - P_U\right)d\,\frac{x}{c}$

c_{x_p} section chord-force coefficient, $\displaystyle\int_{-0.0446}^{0.0554} \left(P_F - P_R\right)d\,\frac{t}{c}$

M   free-stream Mach number

n   airplane normal-load factor

P   pressure coefficient, $\dfrac{p - p_0}{q}$

p   local static pressure, lb/sq ft

p_0 free-stream static pressure, lb/sq ft

q   free-stream dynamic pressure, lb/sq ft

S   wing area, including area projected through fuselage
           (130 sq ft)

t   airfoil-section surface ordinate measured from section
           chord, ft

W   airplane weight, lb

x   chordwise distance from leading edge of section chord, ft

Subscripts:

L   lower surface

U   upper surface

F   forward of upper- or lower-surface maximum ordinate

R   rearward of upper- or lower-surface maximum ordinate

cr   critical (value for which the local flow first becomes sonic)

DESCRIPTION OF AIRPLANE WING

The Bell X-1 research airplane used in these tests and some of the
dimensions are shown in the photograph and three-view drawing presented
as figures 1 and 2. The spanwise and chordwise locations of the pressure-
measuring orifices are shown in figure 3.

The airplane has a wing of aspect ratio 6 and taper ratio 0.5,
with a modified NACA 65-110 airfoil section. Over the flap stations
(stations A and C) the airfoil section was modified rearward of the

85-percent-chord point to give a finite thickness at the trailing edge. For the aileron stations (stations D and F) the cusp was replaced by a straight taper rearward of the 85-percent-chord point to reduce aileron hinge moments (ref. 7). The ordinates of the modified airfoil sections are presented in table I. The 40-percent-chord line is perpendicular to the plane of symmetry, and the wing has an incidence angle with respect to the fuselage axis of 2.5^O at the root and 1.5^O at the tip. The wing was painted and polished during the tests, but no refined filling or smoothing was attempted.

INSTRUMENTATION AND DATA REDUCTION

Standard NACA instrumentation was used to obtain free-stream static pressure, free-stream dynamic pressure, pressure altitude, normal acceleration, and control-surface position. Wing-surface pressures were measured with two NACA recording multiple manometers. All records were synchronized by a common timer.

All surface pressures were measured relative to the pressure in the instrument compartment. The instrument-compartment pressure was measured relative to the static pressure measured by the pitot-static tube, which was corrected to free-stream static pressure by the radar-tracking method of reference 8.

Wing-surface pressures were obtained from 1/8-inch-diameter flush orifices installed in the wing surface. The orifices were connected to the instrument compartment by aluminum tubing of 1/8-inch inside diameter. The length of aluminum tubing varied from about 2 feet at the root station to about 14 feet at the tip station. Approximately 3 feet of rubber tubing of 3/16-inch inside diameter was used to connect each orifice lead to the manometer cell. The effects of lag in the measurement of surface pressures have been neglected since these effects are insignificant at the rates at which the pressures were changing during these tests.

The plots of section pressure distribution obtained throughout the maneuvers, from which the representative pressure-distribution plots of this paper were picked, have been mechanically integrated. Values of section normal-force coefficient, section pitching-moment coefficient (about the quarter-chord point), and section chord-force coefficient were thus obtained throughout the Mach number and normal-force-coefficient range of the tests. Section center-of-pressure locations were calculated from the values of pitching-moment coefficient and normal-force coefficient. Because of the lack of section angle-of-attack data, it was not possible to convert the normal-force and chord-force coefficients to lift and drag coefficients. Also for this reason, none of the data have been presented as a function of angle of attack. The

summary plots of section aerodynamic-characteristic coefficients present these data in the form of cross plots of the initial data, in order that either section normal-force coefficient or Mach number might be held constant.

TESTS

The data presented herein were obtained during unaccelerated stalls at Mach numbers less than 0.50, during a series of pull-ups and push-overs (at approximately constant M) at Mach numbers from 0.53 to 1.19, and during level flight from a Mach number of 0.79 to 1.00. The low-speed data were obtained at altitudes down to about 17,000 feet and the high-speed data were obtained at higher altitudes, up to about 47,000 feet. During all the maneuvers for which data are presented, the rolling velocities were low and the ailerons were held close to neutral. Tabulated data have been presented in references 1 to 4 for many of the specific maneuvers covered in this paper.

ACCURACY

The accuracy of the test results is estimated to be within the following limits:

$$M \ \ldots \ \pm 0.01$$
$$P \ \ldots \ \pm 0.02$$
$$c_n \ \ldots \ \pm 0.05$$
$$c_{m_{c/4}} \ \ldots \ \pm 0.006$$
$$c_{x_p} \ \ldots \ \pm 0.006$$

RESULTS AND DISCUSSION

Pressure Distributions

Representative pressure distributions throughout the normal-force-coefficient and Mach number range of the tests are shown in figures 4 to 7 for the four spanwise stations shown in figure 3(a). The pressure distributions show the characteristic change in shape from the conventional triangular chordwise loading at low speeds to the more nearly rectangular loading at supersonic speeds.

A midsemispan station (station D) was selected as the station most representative of a section having two-dimensional flow; therefore, relatively complete coverage of the normal-force-coefficient and Mach number range was made for this station. To determine the effect of spanwise location on the pressure distribution, less complete tests were made at another midsemispan station (station C), a root station (station A), and a tip station (station F).

Midsemispan stations.- Pressure distributions at station D for low normal-force coefficients are shown in figures 4(a) to 4(c). The shape of the basic pressure distribution as shown in figure 4(b) (where $c_n = 0$) at a Mach number of 0.56 was that of a conventional low-speed pressure distribution for a cambered airfoil. As the Mach number was increased to 0.75 (approximately M_{cr}) the pressure gradient became slightly greater on the upper surface and reached a peak at about 45 percent chord. At a Mach number of 0.82 shocks had formed on both upper and lower surfaces and were located at about 60 to 65 percent chord. With further increase in Mach number the shocks moved steadily rearward, and they reached the trailing edge at a Mach number of about 0.97.

The pressure distributions at normal-force coefficients of -0.20 and 0.20 (figs. 4(a) and 4(c), respectively) showed an ordinary translation of individual pressures from the basic pressure distribution necessary to produce the additional normal force, and a negative pressure peak that developed at a normal-force coefficient of -0.20 near the leading edge on the lower surface.

At a subcritical Mach number a negative pressure peak associated with the expansion around the leading edge developed on the upper surface as a normal-force coefficient of 0.40 was reached, and it increased in magnitude as the normal-force coefficient was increased to 0.80 (figs. 4(d) to 4(f)).

At supercritical Mach numbers the pressure distribution showed large changes in shape with Mach number, attributable to shock formation and movement. The critical Mach number and approximate shock location for various normal-force coefficients (determined by inspection of the pressure-distribution plots) are shown in figure 8. These curves were obtained from the same data from which the representative pressure distributions of figure 4 were selected. The approximate shock location for a section normal-force coefficient of 0.80 is not presented because of insufficient data to define properly the shock location through the Mach number range.

The shock which formed near the leading edge on the upper surface at a slightly supercritical Mach number, in general, moved rearward with increase in Mach number. At a Mach number of about 0.78 the increased

angle of attack necessary to maintain a constant normal-force coefficient resulted in a temporary forward movement of the upper-surface shock, after which the shock progressed steadily rearward and reached the vicinity of the trailing edge at a Mach number of about 0.97. On the lower surface a shock formed at about 60 percent chord at Mach numbers from 0.80 to 0.85. This lower-surface shock moved steadily rearward as the Mach number increased, and reached the trailing edge at a Mach number of about 0.97 at all values of normal-force coefficient tested.

In the range of Mach numbers from 0.83 to 0.92, the upper-surface shock was located forward of the lower-surface shock. This caused a region of reduced loading between the shocks (figs. 4(d) to 4(f)). At a section normal-force coefficient of 0.40 this reduced loading was sufficient to result in negative loading in this region. With both shocks located at the trailing edge (M = 0.97) the loading became approximately rectangular, and further increase in Mach number to 1.19 resulted only in a gradual positive shift in all pressures, so that the shape of the pressure distribution and loading remained relatively unchanged.

Throughout the Mach number range from 0.71 to about 0.89 the reduced pressure recovery rearward of the upper surface shock indicated a region of separated flow (figs. 4(d) to 4(f)). Although the shape of the pressure distributions at normal-force coefficients of 0.60 and 0.80 was generally similar to that at 0.40, the shock locations were not so clearly defined because of more extensive separation at the higher normal-force coefficients. At Mach numbers between about 0.80 and 0.90 the airplane stalled at an angle of attack insufficient to produce a normal-force coefficient of 0.80 at this station (station D).

A comparison has been made in figure 9 of the experimentally determined pressure distributions for station D with theoretical pressure distributions obtained by use of the Theodorsen low-speed method (ref. 9) together with the Prandtl-Glauert compressibility correction. This comparison has been made for a normal-force coefficient of 0.40 at Mach numbers of 0.51, 0.71, and 0.83. As was expected, the comparison shows that at Mach numbers well below critical this theory works well, that it gives a fair approximation up to Mach numbers slightly supercritical, but that it does not satisfactorily predict the shape of the pressure distribution at the higher Mach numbers because of the inability of this theory to predict formation and movement of shocks.

As was anticipated, the pressure distributions at station C (fig. 5) are similar to those at station D, except for small differences in the negative pressure peak at the leading edge and the discontinuity on the lower surface at the leading edge of the flap.

Variation across span.- Data were obtained only to a section normal-force coefficient of 0.70 at the root and tip stations (figs. 6 and 7,

respectively); hence it was not possible to present data for comparison
at the highest normal-force coefficient presented for the midsemispan
stations. The wing first stalls at the root station, and at Mach num-
bers less than about 0.90 a normal-force coefficient of 0.70 is approxi-
mately the maximum normal-force coefficient for that station. It is
apparent that for the tip a normal-force coefficient of 0.70 is not the
maximum but the limit reached on this airplane at Mach numbers less than
0.90. This may be attributed to the fact that, with the reduction in
lift-curve slope due to tip relief and with decreased tip incidence
angle, the airplane angle of attack necessary to reach maximum normal-
force coefficient at the tip is in excess of the angle of attack at
which the airplane stalls.

For a more ready comparison of the shapes of the pressure distribu-
tions across the wing panel, figure 10 is presented to summarize the
pressure distributions at a section normal-force coefficient of 0.40.
To give an indication of the section angle of attack necessary to attain
a normal-force coefficient of 0.40 for a given station, the normal-force
coefficients for the airplane are also shown in figure 10.

At subcritical and slightly supercritical Mach numbers the pressure
distributions show the greatest similarity across the span. The only
significant difference is that a greater negative peak pressure was
reached near the leading edge at the root and tip stations than at sta-
tion D. At Mach numbers from 0.81 to 0.97 the only important difference
in the pressure distributions was in the shock locations and extent of
separation behind the shocks. At a Mach number of approximately 0.81
the upper-surface shock was located at 55 to 60 percent chord at all
stations ($c_n = 0.40$). As the Mach number was increased to about 0.89
the shock at station D had moved forward to 45 percent chord, the shock
at station F had moved rearward to 80 percent chord, and the shock at
station A had apparently remained stationary. As previously mentioned,
the shock at station D temporarily moved forward because of the increased
angle of attack necessary to maintain a constant section normal-force
coefficient. The interference effects of the fuselage and the relieving
effects at the tip apparently reduced the variation of angle of attack
with Mach number for constant normal-force coefficient, to modify the
shock movement in the above manner.

The region of down-load previously discussed for the midsemispan
stations extended inboard to the root station but was diminished slightly.
Because of the more rearward shock location at the tip, a small region
of down-load existed near the trailing edge at a normal-force coeffi-
cient of 0.40 only at Mach numbers near 0.89.

At Mach numbers of 0.81 and 0.89, it may be seen that the flattening
of the pressure gradient behind the shock was greater at station D than

at the root or tip stations, indicating that separation was more severe
at the midsemispan stations.

At a Mach number of 0.97, figure 10 indicates that supersonic flow
existed over all of the wing panel except near the leading edge, and the
pressure distributions at all stations were similar in shape. At the
root and tip stations, however, the loading over the rearward 40 percent
chord was not as great as at the midsemispan stations.

Section Aerodynamic Characteristics

Center of pressure and pitching-moment coefficient.- The variation
with Mach number of the section center-of-pressure location at various
constant values of section normal-force coefficient is shown in figure 11
for each of the four stations. The data for the pitching-moment coeffi-
cient about the quarter-chord point, from which the center-of-pressure
data were obtained, are presented at constant normal-force coefficients
throughout the Mach number range in figure 12. From these figures it
may be seen that rapid changes in section center of pressure and section
pitching-moment coefficient occurred in the Mach number range from
slightly above critical to about 0.96. These changes are apparent
throughout the normal-force range at all spanwise stations and are asso-
ciated with the shock formation and movement formerly discussed.

The midsemispan stations showed a variation of center-of-pressure
location and pitching-moment coefficient with Mach number similar to
that obtained for two-dimensional airfoils. For a level-flight section-
normal-force coefficient ($c_n \approx 0.30$) at stations C and D, it may be seen
that the section center of pressure remained close to the 25-percent-
chord location at Mach numbers up to about 0.70, above which a rearward
shift of center of pressure accompanied the rearward movement of the
upper-surface shock. At a Mach number of 0.83 the center-of-pressure
location had reached about 37 percent chord. At Mach numbers between
0.83 and 0.89 the previously discussed down-load, caused by shock move-
ment, resulted in a forward shift of center of pressure to about 13 per-
cent chord. In the Mach number range from 0.89 to about 0.96 the center
of pressure moved rapidly rearward to about 43 percent chord, because of
the movement of both upper- and lower-surface shocks to near the trailing
edge, where they remained to the limit of the tests. Associated with
this center-of-pressure movement, the section pitching-moment coeffi-
cient changed from a low-speed value of about zero to a value of -0.06
at a Mach number of 0.96 and above, with minimum and maximum values of
-0.04 and 0.04, respectively, in the transonic transition.

At larger section normal-force coefficients (to about 0.70), the
location of the section center of pressure was approximately the same
as that described for the lower lift condition except in the Mach number

range from about 0.75 to 0.96. In this range, as the normal-force coefficient increased the rapid forward and rearward shifting of the center of pressure was diminished. At a normal-force coefficient of 0.70, the center of pressure moved rearward to about 30 percent chord at a Mach number of 0.82 and remained at this point to a Mach number of 0.88 before progressing further rearward. This more gradual shifting of the center of pressure may be attributed to the fact that the pressure recovery through the shock was not so abrupt as at low lift, probably because of development of a family of forked shocks instead of a single normal shock and more extensive separation which left the shock location less well defined. There was a corresponding "softening" of the abrupt changes with Mach number for the pitching-moment coefficients.

At the root and tip stations the variation of section center of pressure and pitching moment with Mach number was similar to that at the midsemispan stations, except that the magnitudes of the variation with Mach number were reduced, especially at the tip section. At the subcritical speeds throughout the lift range the center of pressure at the tip was located at about 25 percent chord, just as at the midsemispan, but at the root the center of pressure was farther forward (about 20 percent chord). At Mach numbers above 0.96, the average center-of-pressure location at the root and tip stations, throughout the lift range, was forward of the location at the midsemispan. The average values were about 37 and 34 percent, respectively, at the root and tip stations, as compared with 43 percent at the midsemispan.

Figure 13 presents, at various constant Mach numbers, the variation of pitching-moment coefficient with normal-force coefficient for the four stations. From the slopes of these curves it may be seen that, for the midsemispan stations, there was a definitely stable variation of section pitching moment for Mach numbers of 0.89 and above. At Mach numbers of 0.83 and below, the midsemispan stations were nearly neutrally stable throughout most of the normal-force-coefficient range. For the root station, at high speeds, a stable variation of pitching-moment coefficient with normal-force coefficient also appeared, but the neutrally stable condition was approached as Mach number was diminished to 0.89, and at Mach numbers of 0.83 and below there was a slightly unstable variation. The tip station also showed a stable variation at the higher Mach numbers. As the Mach number was decreased to about 0.75, the variation gradually approached a neutrally stable condition, which remained to lower speeds.

Chord-force coefficient.- The variation with Mach number of section chord-force coefficient is shown in figure 14. At all stations and all values of section normal-force coefficient similar trends are shown. At a given normal-force coefficient an approximately constant negative (forward) chord-force coefficient existed at subsonic Mach numbers up to somewhat above M_{cr}. At transonic Mach numbers a relatively

steady increase in chord-force coefficient occurred, and it continued to
a definitely positive (rearward) value at Mach numbers approaching 1.0,
above which the values remained nearly constant to the limit of the
tests. At the lower Mach numbers the magnitude of the negative chord-
force coefficient increased steadily with normal-force coefficient
because of the increasing negative pressure peak near the leading edge.
The change to positive chord-force coefficients in the transonic Mach
number region for all normal-force coefficients presented may be attrib-
uted to a decrease of the leading-edge negative-pressure peak with
increasing Mach number, and also to the increasing magnitude of negative
pressures over the rearward part of the upper surface. The only signif-
icant difference in the chord-force coefficient across the wing panel
was the Mach number at which the curves reached the maximum value
(approximately 0.92 at the tip and 0.96 across the rest of the span).

CONCLUSIONS

Results of chordwise pressure-distribution measurements over four
spanwise stations of the wing of the Bell X-1 research airplane show
that:

1. The pressure distributions at the four spanwise stations were
generally similar at comparable section normal-force coefficients, and
showed a change from the conventional low-speed triangular chordwise
loading to the more nearly rectangular loading at supersonic speeds.

2. Large changes in the shape of the pressure distributions, with
accompanying movement of the section center of pressure, occurred at
Mach numbers from about 0.80 to 0.96 at the midsemispan station as a
result of shock movement with a change in Mach number. The trends of
center-of-pressure movement at the root and tip stations were the same
as at the midsemispan stations, but were not so pronounced because of
fuselage and tip effects. The most abrupt center-of-pressure shift
occurred at low lift at the root and midsemispan stations, where a for-
ward movement to about 15 percent chord occurred at a Mach number of
0.89.

3. There was a definitely stable variation of section pitching-
moment coefficient with section normal-force coefficient at Mach num-
bers of 0.89 and above for each of the four spanwise stations.

4. At Mach numbers between 0.81 and 0.89, the reduction of pressure
recovery behind the shock was greater at the midsemispan stations than
at the root or tip stations. This result indicated that separation was
more severe at the midsemispan stations.

5. At a given section normal-force coefficient an approximately constant negative (forward) chord-force coefficient existed at subsonic Mach numbers up to somewhat above the critical Mach number at all stations. At transonic Mach numbers a relatively steady increase in chord-force coefficient occurred, and it continued to a definitely positive value at Mach numbers approaching 1.0, above which the values remained nearly constant to the limit of the tests.
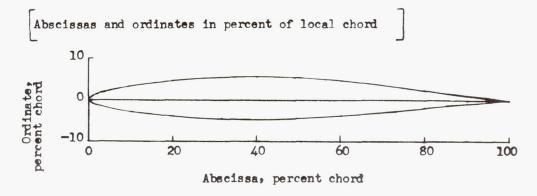
Langley Aeronautical Laboratory,
      National Advisory Committee for Aeronautics,
            Langley Field, Va.

REFERENCES
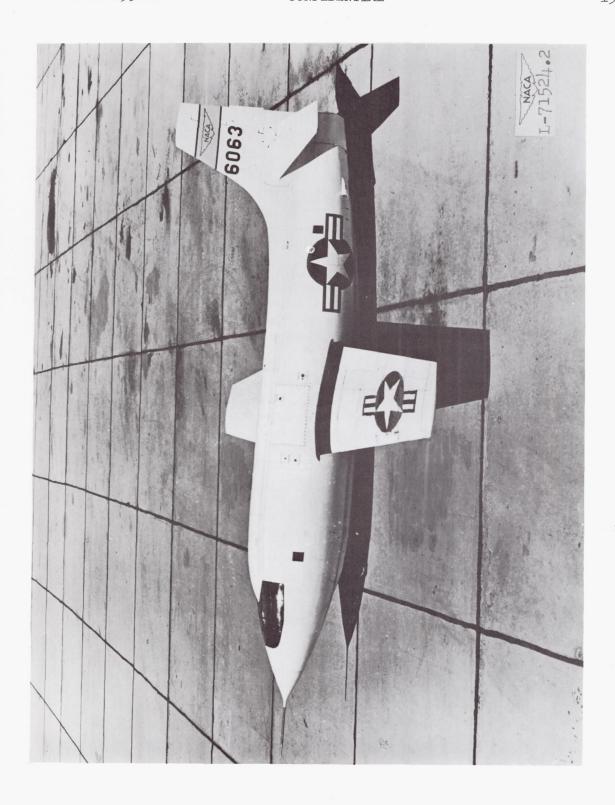
1. Carner, H. Arthur, and Payne, Mary M.: Tabulated Pressure Coefficients and Aerodynamic Characteristics Measured on the Wing of the Bell X-1 Airplane in Level Flight at Mach Numbers From 0.79 to 1.00 and in a Pull-Up at a Mach Number of 0.96. NACA RM L50H25, 1950.

2. Knapp, Ronald J., and Wilken, Gertrude V.: Tabulated Pressure Coefficients and Aerodynamic Characteristics Measured on the Wing of the Bell X-1 Airplane in Pull-Ups at Mach Numbers From 0.53 to 0.99. NACA RM L50H28, 1950.

3. Smith, Lawrence A.: Tabulated Pressure Coefficients and Aerodynamic Characteristics Measured on the Wing of the Bell X-1 Airplane in an Unaccelerated Stall and in Pull-Ups at Mach Numbers of 0.74, 0.75, 0.94, and 0.97. NACA RM L51B23, 1951.

4. Knapp, Ronald J.: Tabulated Pressure Coefficients and Aerodynamic Characteristics Measured on the Wing of the Bell X-1 Airplane in an Unaccelerated Low-Speed Stall, in Push-Overs at Mach Numbers of 0.83 and 0.99, and in a Pull-Up at a Mach Number of 1.16. NACA RM L51F25, 1951.

5. Carner, H. Arthur, and Knapp, Ronald J.: Flight Measurements of the Pressure Distribution on the Wing of the X-1 Airplane (10-Percent-Thick Wing) Over a Chordwise Station Near the Midspan, in Level Flight at Mach Numbers From 0.79 to 1.00 and in a Pull-Up at a Mach Number of 0.96. NACA RM L50H04, 1950.

6. Beeler, De E., McLaughlin, Milton D., and Clift, Dorothy C.: Measurements of the Chordwise Pressure Distributions Over the Wing of the XS-1 Research Airplane in Flight. NACA RM L8G21, 1948.

7. Ormsby, C. A.: Aerodynamic Design of the MX-653 Wing. Rep. No. 44-943-008, Bell Aircraft Corp., June 5, 1945.

8. Zalovcik, John A.: A Radar Method of Calibrating Airspeed Installations on Airplanes in Maneuvers at High Altitudes and at Transonic and Supersonic Speeds. NACA Rep. 985, 1950. (Supersedes NACA TN 1979.)

9. Theodorsen, Theodore: Theory of Wing Sections of Arbitrary Shape. NACA Rep. 411, 1931.

TABLE **I**

AIRFOIL PROFILE AND ORDINATES OF THE BELL X-1 WING

$$\left[\text{Abscissas and ordinates in percent of local chord} \right]$$

Abscissa, percent chord

Modified NACA 65-110 airfoil section					
Upper surface			Lower surface		
Abscissa	Ordinate		Abscissa	Ordinate	
	Flap stations	Aileron stations		Flap stations	Aileron stations
0	0	0	0	0	0
.468	.796	.796	.533	-.746	-.746
.714	.966	.966	.786	-.896	-.896
1.210	1.222	1.222	1.290	-1.115	-1.115
2.454	1.667	1.667	2.546	-1.481	-1.481
4.949	2.334	2.334	5.051	-2.018	-2.018
7.447	2.859	2.859	7.553	-2.435	-2.435
9.947	3.298	3.298	10.053	-2.781	-2.781
14.949	4.002	4.002	15.051	-3.329	-3.329
19.954	4.541	4.541	20.046	-3.745	-3.745
24.961	4.951	4.951	25.039	-4.056	-4.056
29.968	5.246	5.246	30.032	-4.274	-4.274
34.976	5.439	5.439	35.024	-4.409	-4.409
39.984	5.532	5.532	40.016	-4.461	-4.461
44.992	5.511	5.511	45.008	-4.416	-4.416
50.000	5.364	5.364	50.000	-4.261	-4.261
55.007	5.078	5.078	54.993	-3.983	-3.983
60.013	4.682	4.682	59.987	-3.611	-3.611
65.018	4.197	4.197	64.982	-3.167	-3.167
70.021	3.642	3.642	69.979	-2.670	-2.670
75.023	3.032	3.032	74.977	-2.137	-2.137
80.022	2.385	2.385	79.978	-1.589	-1.589
85.019	1.721	1.721	84.981	-1.048	-1.048
90.000	1.100	1.148	90.000	-.687	-.698
95.000	.525	.574	95.000	-.295	-.349
100.000	.010	0	100.000	-.010	0
L. E. radius : 0.687 percent chord					

Figure 1.- Bell X-1 airplane.
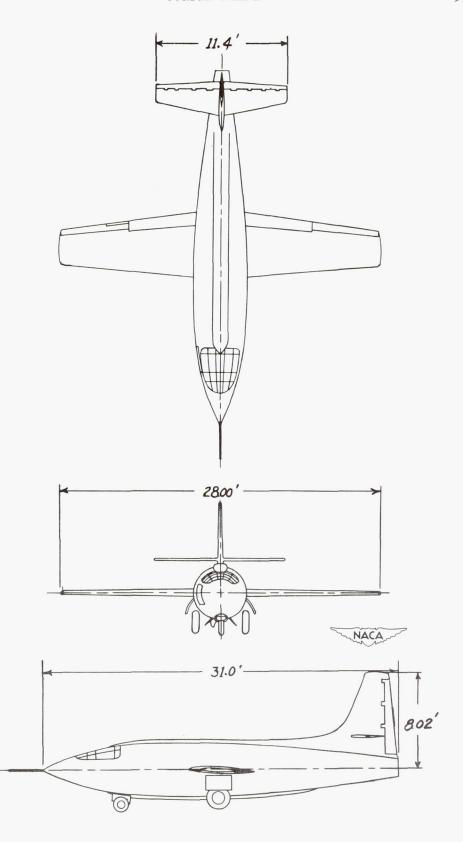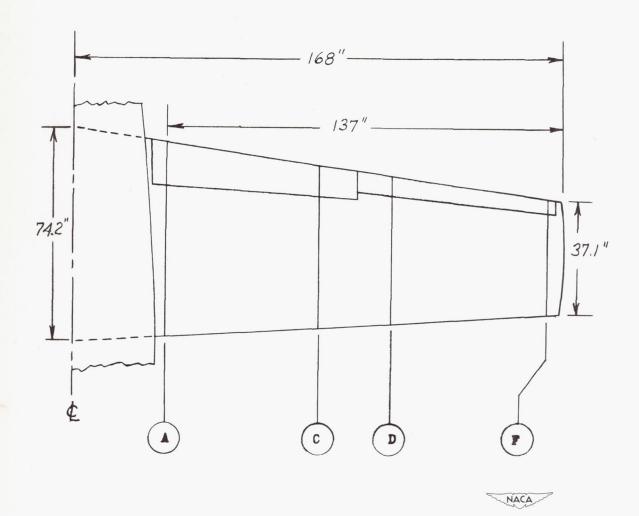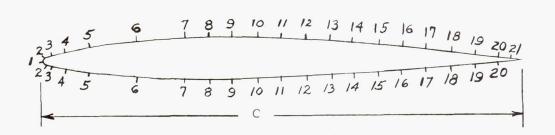
Figure 2.- Three-view drawing of X-1 airplane.

Span station	A	C	D	F
Distance from airplane $\bar{\text{C}}$, percent b/2	18.5	49.1	64.4	95.1

(a) Spanwise.
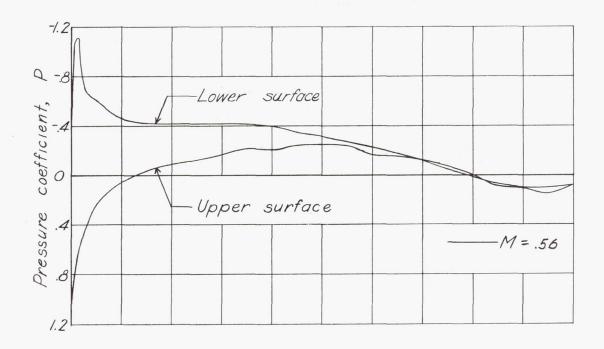
Figure 3.- Spanwise and chordwise locations of pressure-measuring orifices.
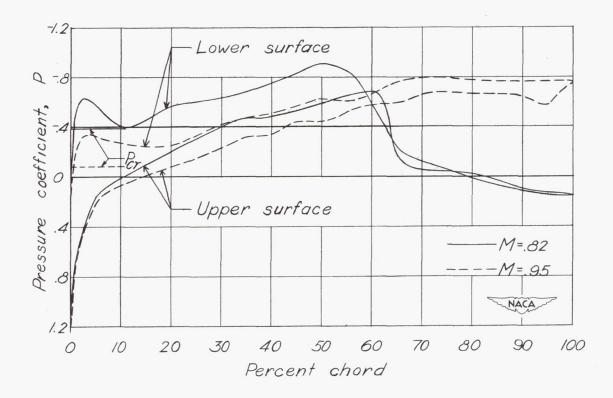
Orifice station location, percent chord								
Span station	A		C		D		F	
Orifice	Upper	Lower	Upper	Lower	Upper	Lower	Upper	Lower
1	0	0	0	0	0	0	0	0
2	1.16	1.16	1.18	1.28	1.29	1.38	1.16	1.23
3	2.40	2.40	2.40	2.40	2.66	2.66	2.64	2.39
4	4.79	4.79	5.04	5.04	5.16	5.16	5.49	5.03
5	9.85	9.98	9.64	9.64	10.95	10.95	10.42	10.16
6	19.75	19.92	20.00	20.00	19.76	20.10	19.92	19.66
7	29.80	30.00	29.32	30.00	30.00	30.00	29.75	29.62
8	34.85	35.05	34.78	35.20	34.80	35.10	35.05	35.05
9	40.00	40.10	39.58	40.00	40.00	40.15	40.07	40.07
10	45.10	45.00	44.40	45.92	45.15	45.35	45.00	45.00
11	50.20	49.70	49.52	50.18	50.18	50.30	50.02	50.00
12	54.90	54.90	55.10	55.20	55.28	55.28	55.05	54.95
13	60.38	60.00	59.90	60.00	60.80	60.60	59.70	60.00
14	65.00	65.00	65.00	65.00	65.40	65.60	64.95	64.95
15	70.00	70.00	70.00	70.00	69.85	69.95	70.05	70.05
16	74.10	74.42	74.00	74.38	74.40	74.20	73.85	74.30
17	78.60	78.60	78.00	78.20	79.50	79.70	79.85	80.05
18	84.90	85.08	84.95	84.95	85.62	85.40	85.70	85.70
19	90.00	90.00	90.00	90.00	90.00	90.00	89.60	89.60
20	94.80	94.80	95.00	95.10	95.00	95.00	95.10	95.30
21	97.65	———	97.30	———	97.10	———	96.10	———

(b) Chordwise.
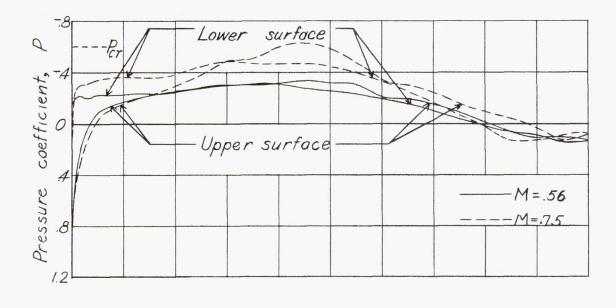
Figure 3.- Concluded.
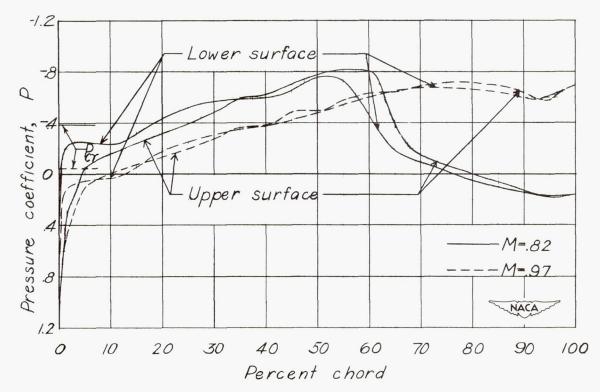
(a) $c_n = -0.20$.
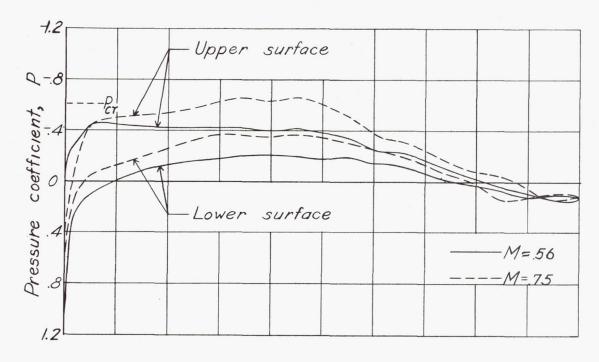
Figure 4.- Mach number effects on the chordwise pressure distributions at station D of the 10-percent-thick wing of the Bell X-1 airplane.
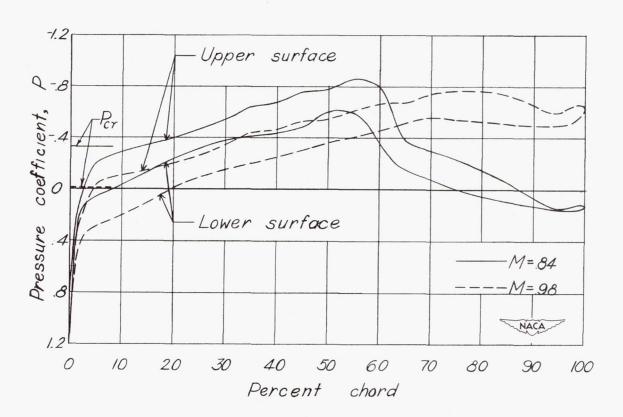
(b) $c_n = 0$.
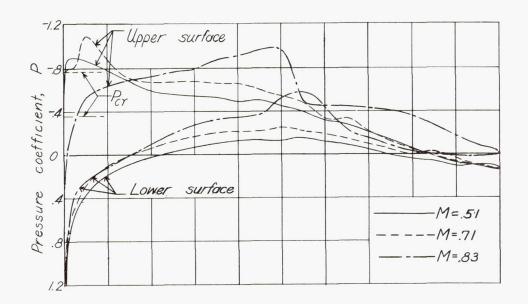
Figure 4.- Continued.
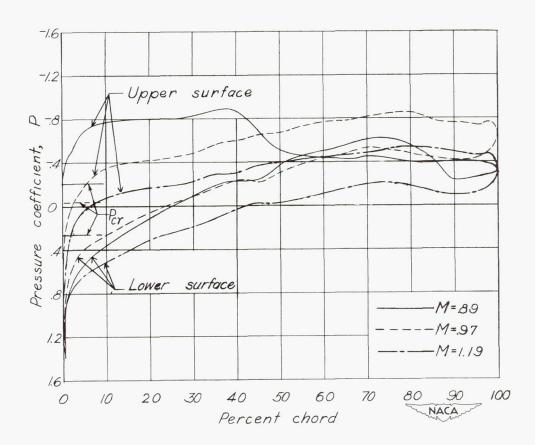
(c) $c_n = 0.20$.
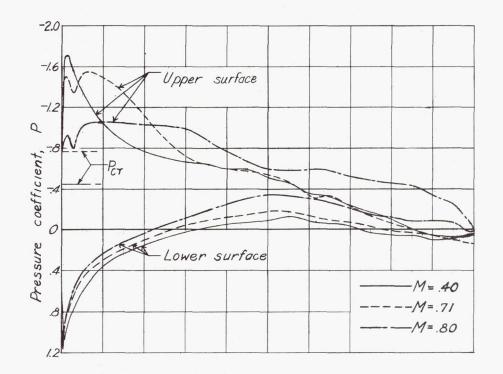
Figure 4.- Continued.
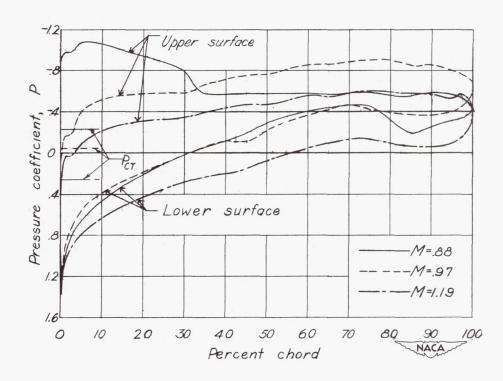
(d) $c_n = 0.40$.
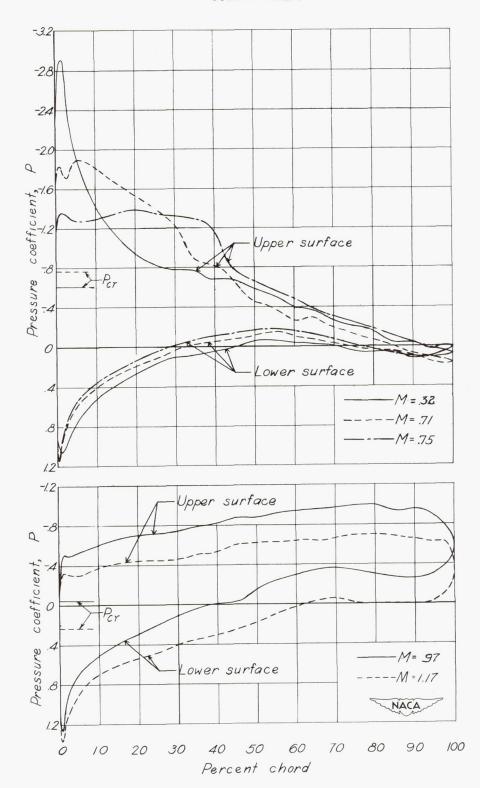
Figure 4.- Continued.
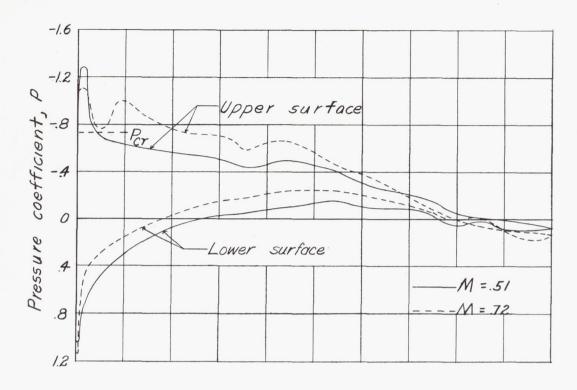
(e) $c_n = 0.60$.
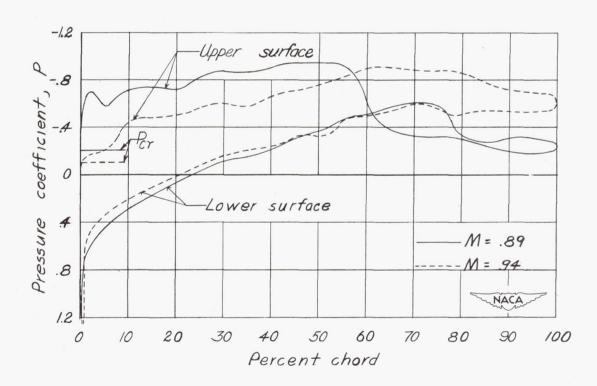
Figure 4.- Continued.

(f) $c_n = 0.80$.
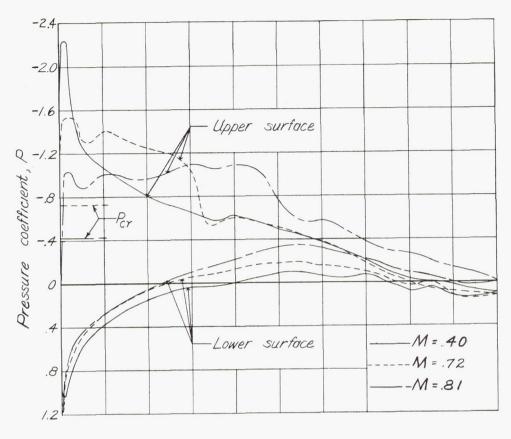
Figure 4.- Concluded.
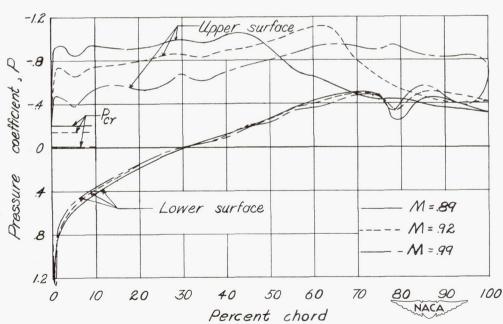
(a) $c_n = 0.40$.
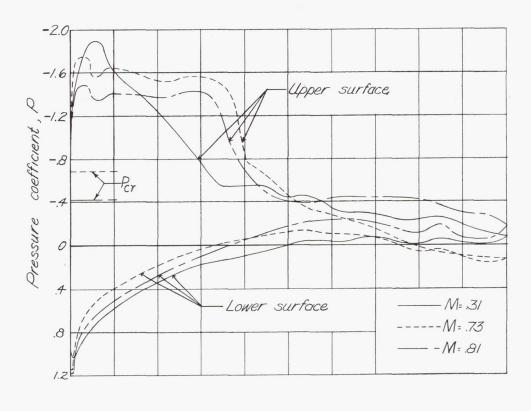
Figure 5.- Mach number effects on the chordwise pressure distributions at station C of the 10-percent-thick wing of the Bell X-1 airplane.

CONFIDENTIAL   NACA RM L53D20
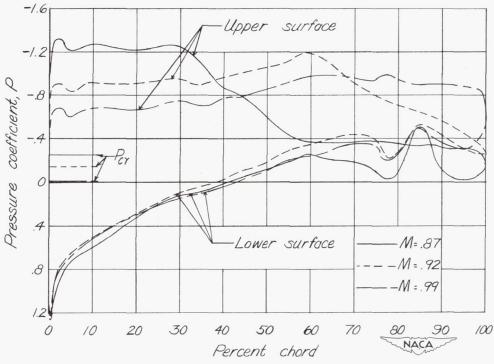
(b) $c_n = 0.60$.
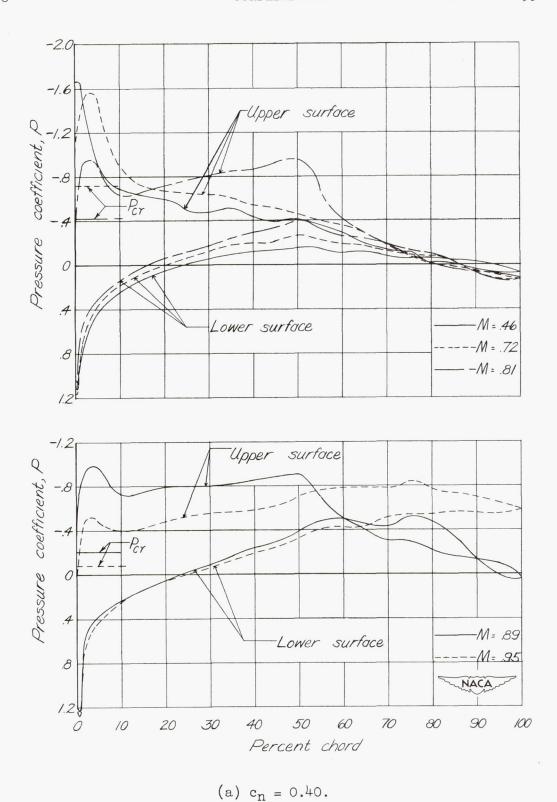
Figure 5.- Continued.

CONFIDENTIAL
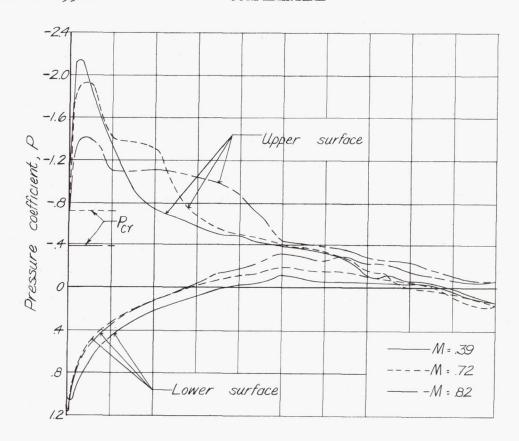
(c) $c_n = 0.80$.
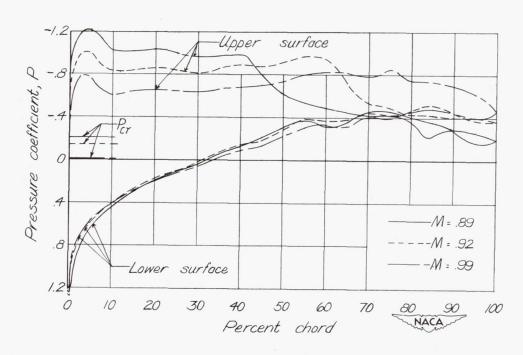
Figure 5.- Concluded.

(a) $c_n = 0.40$.
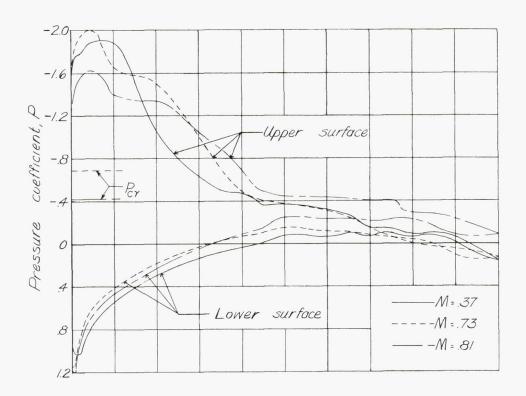
Figure 6.- Mach number effects on the chordwise pressure distributions at station A of the 10-percent-thick wing of the Bell X-1 airplane.
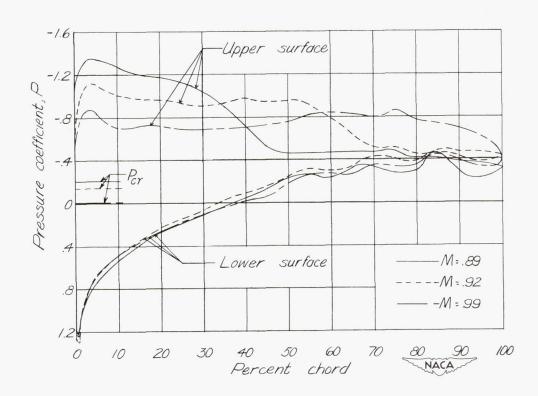
(b) $c_n = 0.60$.
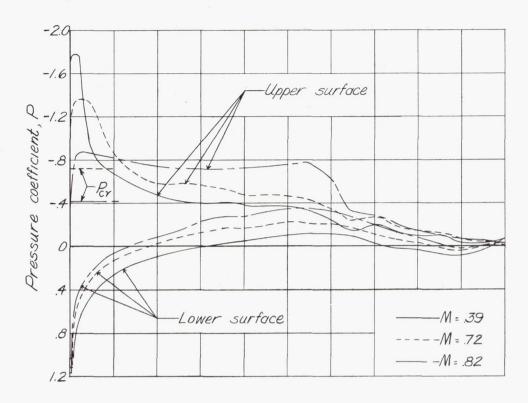
Figure 6.- Continued.

(c) $c_n = 0.70$.

Figure 6.- Concluded.

(a) $c_n = 0.40$.
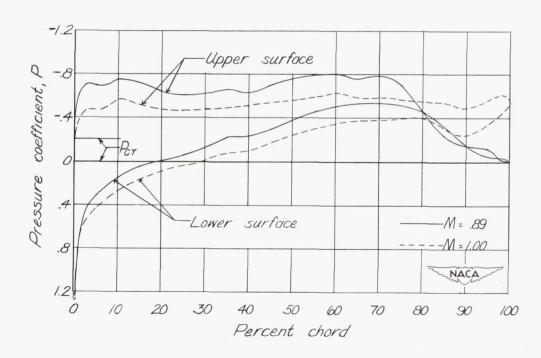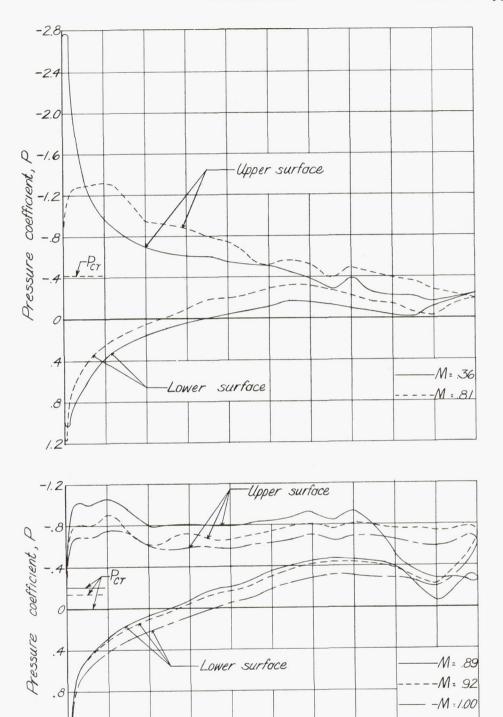
Figure 7.- Mach number effects on the chordwise pressure distributions at station F of the 10-percent-thick wing of the Bell X-1 airplane.

(b) $c_n = 0.60$.

Figure 7.- Continued.
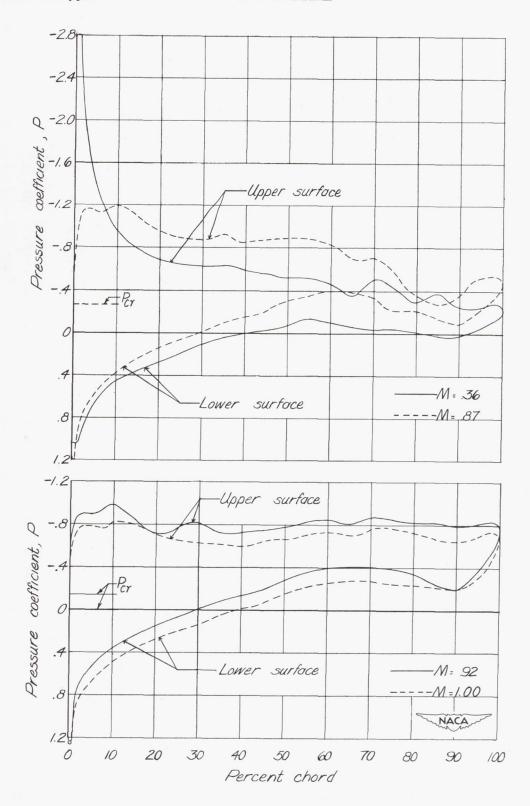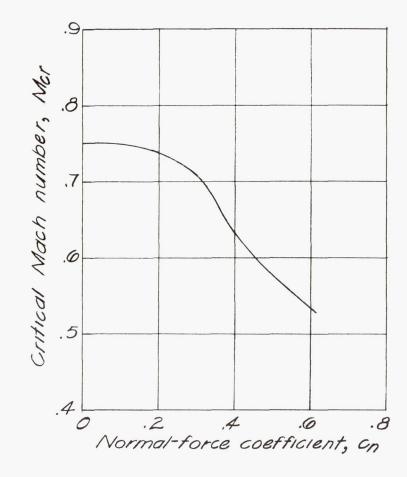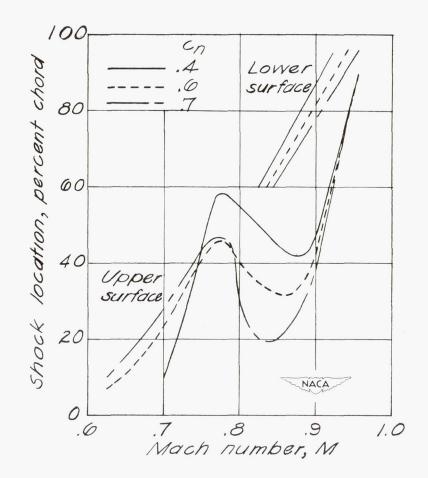
(c) $c_n = 0.70$.

Figure 7.- Concluded.

(a) Critical Mach number.

(b) Approximate shock location.

Figure 8.- Critical Mach number and approximate shock location for wing
station D at various values of section normal-force coefficient.
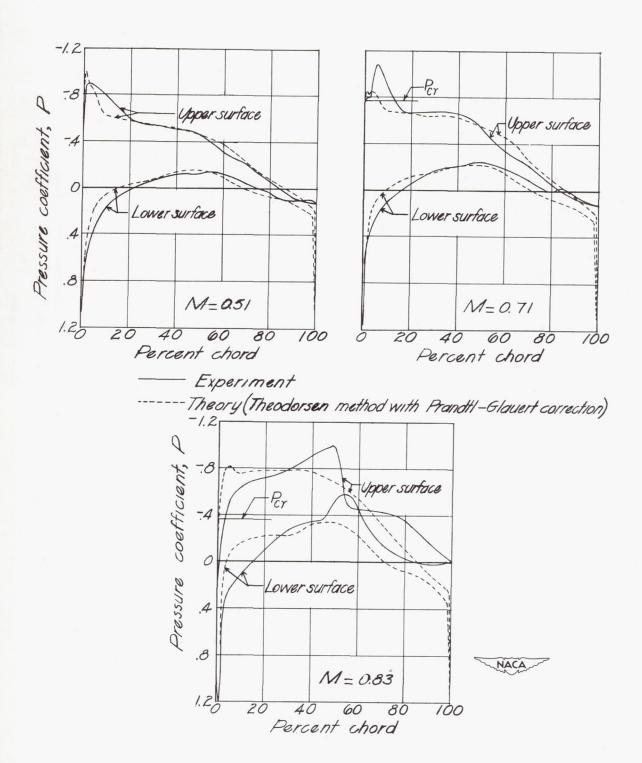
Figure 9.- Comparison of theory with experimentally determined pressure distributions at station D. $c_n = 0.4$.
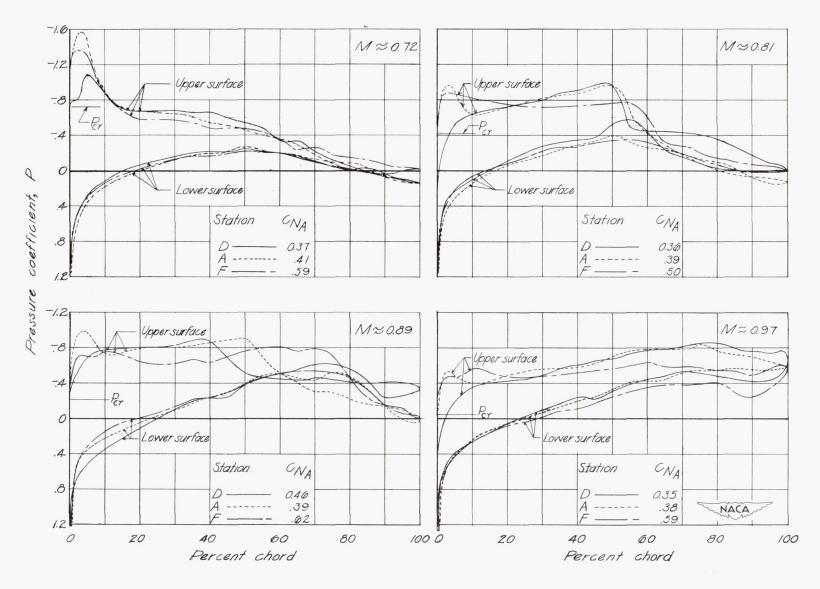
Figure 10.- Comparison of pressure distributions measured at midsemispan, root, and tip stations for various Mach numbers. $c_n = 0.4$.
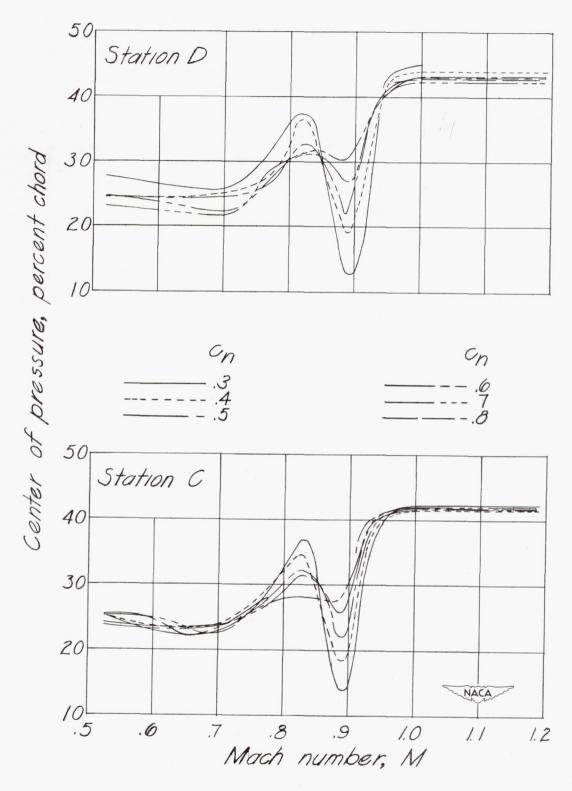
Figure 11.- Variation of section center of pressure with Mach number at various values of section normal-force coefficient for four spanwise stations.
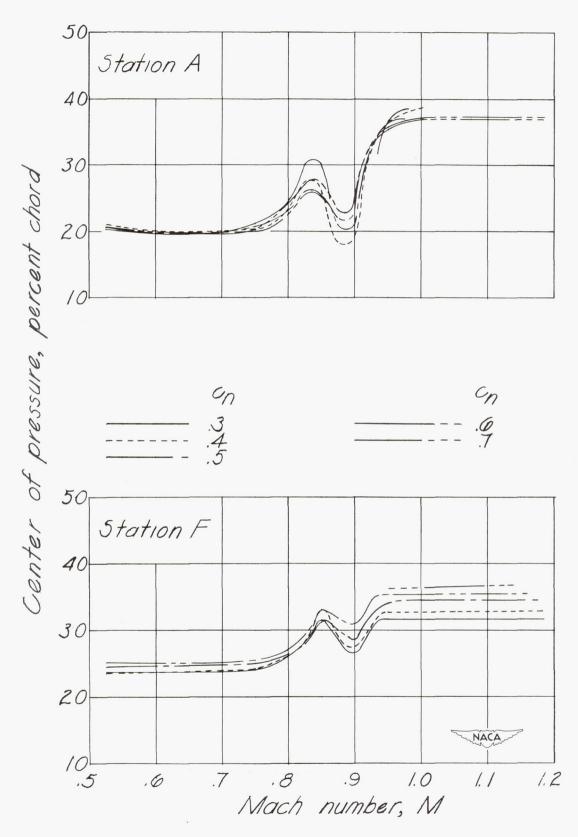
Figure 11.- Concluded.
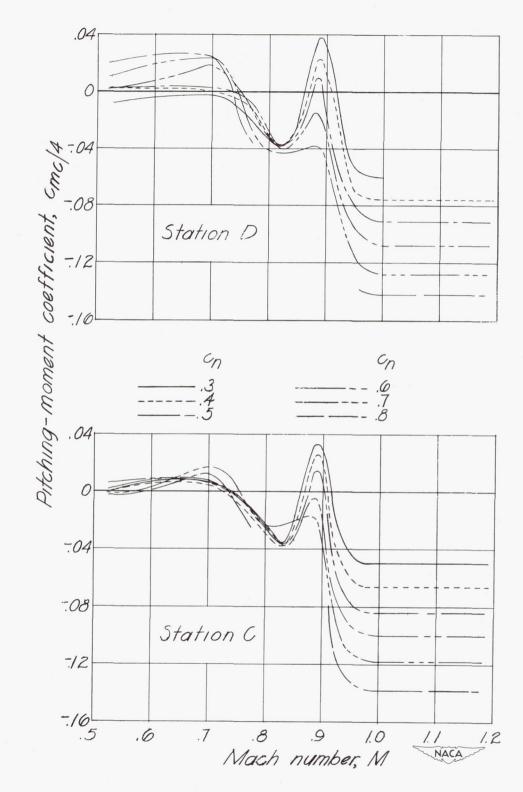
Figure 12.- Variation of section pitching-moment coefficient with Mach number at various values of section normal-force coefficient for four spanwise stations.
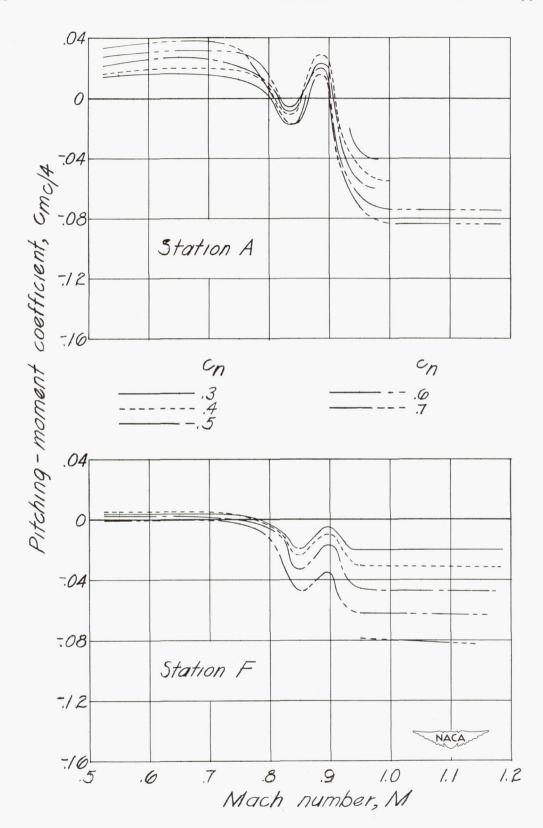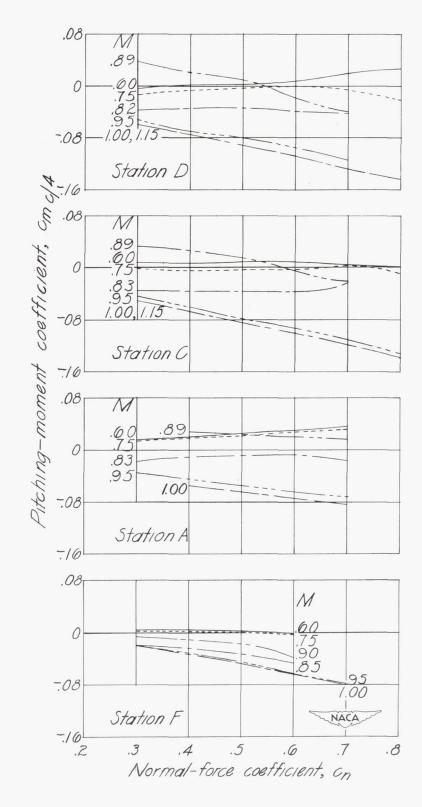
Figure 12.- Concluded.

Figure 13.- Variation of section pitching-moment coefficient with section
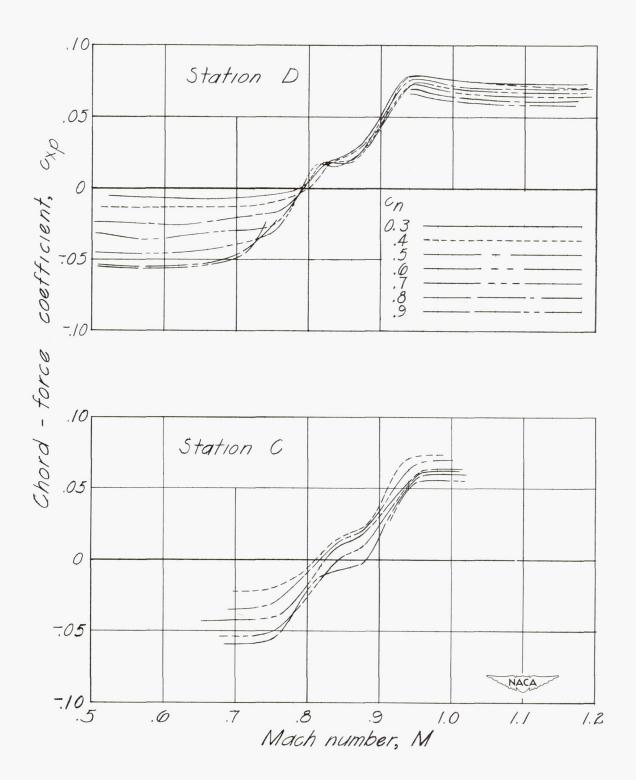normal-force coefficient at various Mach numbers for four spanwise
stations.

Figure 14.- Variation of section chord-force coefficient with Mach number at various section normal-force coefficients for four spanwise stations.
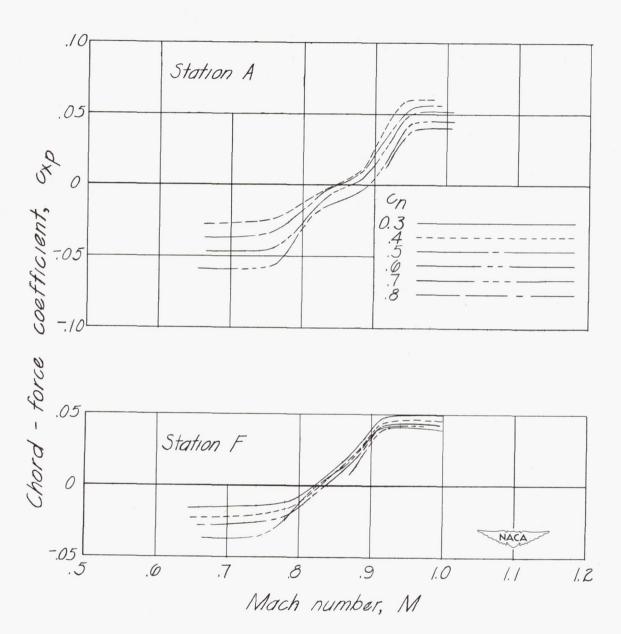
Figure 14.- Concluded.